Performance of Nonlinear Receivers in Asynchronous Spectral-Phase-Encoding Optical CDMA Systems

Bin Ni, James S. Lehnert, *Fellow, IEEE*, and Andrew M. Weiner, *Fellow, IEEE*

***Abstract*—Because of limits on the speed of the photodetector, a nonlinear thresholder is needed at the receiver of a spectral-phase-encoding optical code-division multiple-access system to discriminate between the correctly decoded short pulse and the low-intensity interference. The two most common nonlinear receivers based on second harmonic generation and self-phase modulation effects are analyzed in this paper. Mathematical models are provided, and analytical results are obtained to estimate the receivers' performances. Numerical simulations are carried out for both receivers with different system parameters. Both m-sequences and random binary codes are examined for spreading. The results provide a profile of how these nonlinear receivers perform with various system settings. It is found that, when an m-sequence is used as the spreading code, the encoded signal does not obey Gaussian statistics, and the system performs better than an equivalent system using a random code.**

***Index Terms*—Nonlinear receiver, optical code-division multiple access (OCDMA), second harmonic generation (SHG), self-phase modulation (SPM).**

I. Introduction

CODE-DIVISION multiple access (CDMA) has been a successful technology in wireless communication since the latter half of the last century. People started to transplant it to optical communication systems in the 1970s in order to build high-speed, asynchronous, and secure communication networks [1]. As in wireless CDMA systems, the transmitted information in an optical CDMA (OCDMA) system is encoded into pseudo-random signals with bandwidth much larger than the data rate. Signals from all transmitters overlap in both time and frequency. Only the intended receiver with the matching code sequence can decode the signal from a particular transmitter and recover the data. Signals from all other transmitters become multiple-access interference (MAI), which corrupts the desired signal. One of the most important tasks of designing an OCDMA system is to suppress the MAI as much as possible. OCDMA schemes are classified as incoherent or coherent depending on whether the encoding and decoding processes [2] make use of the coherence in the light source. Coherent schemes [3]–[6] manipulate the field of the light pulses by altering its phase. Incoherent schemes, on the other hand, disregard the coherence and only utilize the power of the optical signal. Incoherent systems are sometimes regarded as more practical because of their low complexity. Coherent systems achieve higher performance than the incoherent ones, but may require more expensive light sources and high-precision control of the optical path within the encoder and decoder. As one of the earliest schemes for coherent OCDMA, the ultrashort-pulse spectral-phase-encoding (SPE) technique was proposed in [7]. A mode-locked laser is used as the broadband coherent light source. The encoder and decoder are implemented with the 4-f lens-grating apparatus. A phase mask is placed at the center focal plane, and different frequency components of a short pulse experience different phase shifts in the encoder. The encoded signal is broadened and becomes noise-like in the time domain. At the receiver, the decoder simply compensates the phase offset introduced by the encoder and recovers the original short pulse. This scheme is often referred to as the SPE or the coherent-ultrashort-pulse (CUP) scheme. With the recent developments of optical devices, some other techniques have been used to accomplish this encoding and decoding process. In [4], the multipath glass substrate is used in place of the grating to achieve higher resolution. Two other research groups have reported [5], [9] using the superstructured fiber Bragg grating as the encoder and decoder. The performance of the SPE scheme is studied analytically in [3] with the assumptions of a random binary spreading code, asynchronous operation between different users, and an ideal ultrafast nonlinear optical thresholder, which is able to respond to the instantaneous power of the pulse.

We first examine the need for a nonlinear optical thresholder. The fastest commercial photodetectors (PDs) have response times around 9 ps, which are much longer than the pulse durations used in many of the reported experiments. The response times of most practical PDs are equal to, or longer than, the encoded-signal length. This is also true of most electronics available for use in the decision circuit subsequent to the PD. Since the encoded signal has the same amount of energy as the uncoded short pulse, the responses of a PD and subsequent electronics to a short pulse and an incorrectly decoded MAI are the same. This problem was illustrated by Jiang *et al.* in [13]. Hence, some nonlinear device has to be used in the receiver to discriminate between the recovered short pulse and the MAI. In [15], a receiver that uses the self-phase-modulation (SPM) effect in a dispersion-shifted fiber is demonstrated.

Manuscript received April 13, 2006; revised October 10, 2006.

B. Ni was with the School of Electrical and Computer Engineering, Purdue University, West Lafayette, IN 47907-2035 USA. He is now with Marvell Semiconductor, Santa Clara, CA 95054 USA.

J. S. Lehnert and A. M. Weiner are with the School of Electrical and Computer Engineering, Purdue University, West Lafayette, IN 47907-2035 USA.

Color versions of one or more of the figures in this paper are available online at http://ieeexplore.ieee.org.

Digital Object Identifier 10.1109/JLT.2007.901338

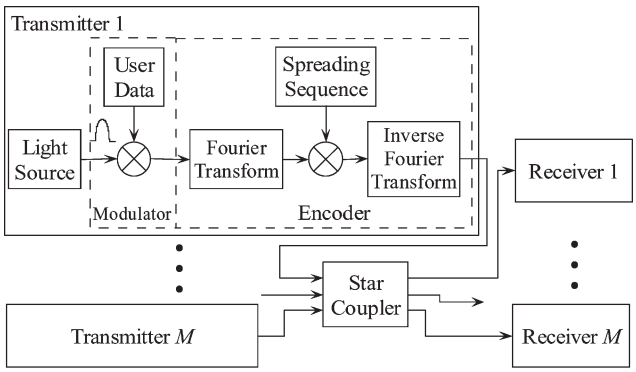

Fig. 1. CUP SPE OCDMA system.

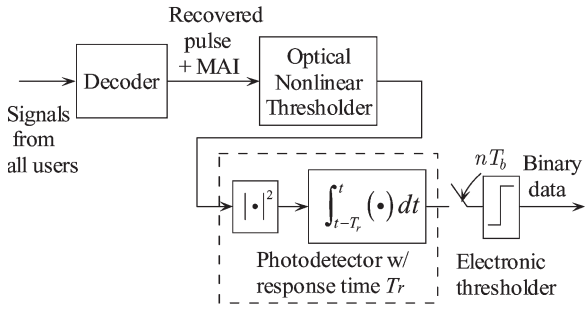

Fig. 2. Nonlinear receiver structure.

Wang *et al.* [9]–[11] recently improved this receiver by making use of the supercontinuum (SC) effect. Scott *et al.* [16]–[20] at the University of California have implemented a high-speed multiuser testbed using highly nonlinear fiber (HNLF) as the thresholder. References [12]–[14] showed the possibility of using the second-harmonic-generation (SHG) effect to realize the receiver. In both receiver structures, the nonlinear effects generate some strong new frequency components for the short pulse, while the spectrum of the low-intensity MAI is barely changed. An optical filter is placed after the nonlinear medium to pass only the new frequencies. Hence, a strong contrast is seen by the PD between the interference and the desired signal.

Due to the limitations of cost and complexity, it is difficult to implement a large number of independent users in the laboratory. In all the reported OCDMA experiments, the number of users was limited to at most 12 [11], [16], with a single light source. It is also difficult to test the system performances in the laboratory with different settings. Therefore, it is interesting to model the performance of these nonlinear receivers with a large number of users and different parameters. In this paper, both the SHG-based and the SPM-based receivers are modeled and analyzed. Performances for different walk-off lengths for the SHG-based receiver and different modulation strengths for the SPM-based receiver are evaluated. Random binary sequences and m-sequences are examined as the spreading codes. In this paper, total asynchrony is assumed across different users, i.e., no efforts have been made to coordinate the timing of the signals from different transmitters. This is one of the claimed advantages of using CDMA in optic fibers [2]. However, in order to reduce MAI, many experiments are moving toward the synchronous case [12]–[14], [16]–[20], which requires complex control of timing. The performance of synchronous OCDMA systems is not considered in this paper.

The next section provides a description of the system model, including the receiver structures. The analyses of the system performances are provided in Section III. The numerical simulations and the results are presented in Section IV. The last section concludes this paper.

II. Description of the System Model

The block diagram of a CUP OCDMA system is shown in Fig. 1. A mode-locked laser is used to generate an ultrashort pulse train at a repetition rate equal to the data bit rate. ON–OFF keying is first applied by a modulator, which only allows a light pulse to pass when "1" is transmitted. Nothing comes from the transmitter when the data bit is "0." The encoder first separates the optical frequencies (equivalent to taking a Fourier transform of the incoming light) and shifts the phases of selected frequency components by π. The pattern of the phase-shifting mask is determined by the spreading sequence assigned to the transmitter. After recombination by the second grating, which is equivalent to an inverse Fourier transform, a pseudorandom light signal is generated at the output. The length of the encoded signal is N_0 times longer than the original pulse duration, and the intensity is reduced by the same factor, where N_0 is the length of the spreading code [3]. Signals from different users are added and distributed to all receivers by the star coupler. The diagram of the receiver structure is shown in Fig. 2. The decoder in a receiver has a setup similar to the encoder in the transmitter. It compensates for the phase shifts introduced by the desired transmitter and recovers the original short pulse. The signals from other transmitters remain noise-like and low in power. They become the MAI that results in a bit-error rate (BER) floor. This BER floor, which is caused by MAI, cannot be overcome by increasing the power of the transmitters. In this paper, it is assumed that the transmitted power is large enough such that any other noise can be ignored relative to the MAI. The system performance is limited by the MAI only.

Ideally, an ultrafast optical thresholder is placed after the decoder. If the instantaneous optical power of the decoded light signal exceeds some threshold value, the light is transmitted; otherwise, the light is assumed to be completely suppressed. An electronic decision circuit then detects the data bit by integrating the optical power passed by this ideal thresholder over the response time of the electronics. The performance of this receiver is analyzed in [3], both for the ideal case, where the electronics response time is equal to the duration of the decoded pulse, and for the practical case, where the electronics response time is longer. This receiver structure is shown in Fig. 2. Note, however, that an ideal ultrafast optical thresholder has never been demonstrated. Instead, experiments use practical nonlinear optical devices, which do pass more energy for the correctly decoded short pulse than for the low-intensity MAI, but do not provide the ideal behavior described above. In this paper, we model the case of OCDMA receivers using nonlinear optical devices based on either SHG or SPM. Following the nonlinear optical device, the PD is taken to have response time T_r;

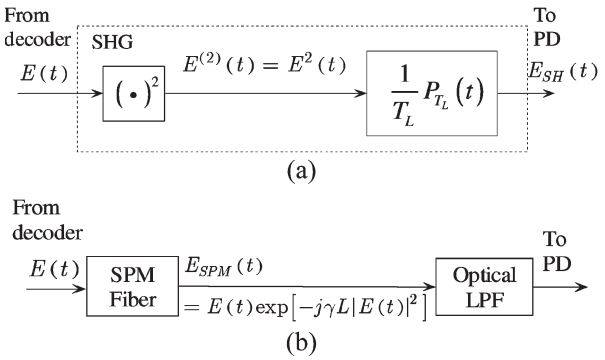

Fig. 3. Structures of the nonlinear optical thresholders. (a) SHG-based optical thresholder. $P_{T_L}(t) = 1$ for $0 \le t \le T_L$ and $P_{T_L}(t) = 0$ for elsewhere. (b) SPM-based optical thresholder.

therefore, we model the PD as an ideal square-law converter (power detector) followed by a sliding integrator over time interval T_r. The output of the integrator is the optical energy within the preceding response time. This model is equivalent to a squaring device followed by a linear filter with a rectangular impulse response. If T_r is greater than or equal to the encoded-signal length, the PD alone (i.e., without the nonlinear optical device) cannot be used to discriminate between the recovered pulse and the equally energetic MAI from another user.

The block diagram of the SHG-based nonlinear thresholder is depicted in Fig. 3(a). An SHG crystal, such as period-poled lithium niobate, is placed between the decoder and the PD. The behavior of the SHG effect is discussed in depth in [21]. In our model, the electric field of the input fundamental signal gets squared by the first stage and is applied to the input of a filter with a rectangular impulse response. The output is the electric field of the second-harmonic (SH) signal. The filter reflects the walk-off effect introduced by the group velocity mismatch (GVM) between the fundamental pulse and the SH pulse. It is modeled to have a rectangular impulse response with length T_L and amplitude $1/T_L$. The parameter T_L is determined by

$$T_L = L|\alpha| \tag{1}$$

where L is the length of the nonlinear crystal, and $\alpha = 1/v_{g_1} - 1/v_{g_2}$ is the GVM. When a thin crystal is used, T_L is much smaller than the pulse duration, and the filtering effect can be ignored. When the crystal is thick and T_L is larger than the pulse duration, the SHG signal is broadened in the time domain and is bandpass filtered in the frequency domain. In the theoretical analysis in the next section, a thin crystal is assumed. A thick crystal is considered in the simulation. Such thick SHG crystals have been shown to allow very strong rejection of improperly decoded signals in single-user operation [12] and to allow operation at very low power. This is important for scaling to a large number of users [13], [14]. The optical carrier frequency is doubled by the SHG. A PD working at twice the fundamental carrier frequency has to be used to detect the SH signal. When "1" is sent by the desired transmitter, the energy of the SH signal, which is caused by the recovered short pulse, is much stronger than that caused by the low-intensity MAI only. Hence, the output of the PD is quite different for the two bits.

The structure of the SPM-based nonlinear thresholder is shown in Fig. 3(b). The SPM effect couples the signal amplitude into the phase of the signal and thus generates new frequency components (this effect is discussed in detail in [22]). If the fiber is relatively short, such that the group velocity dispersion can be ignored, then the mathematical model for the SPM effect can be described by the simple equation given by

$$E_{\mathrm{SPM}}(t) = E_{\mathrm{in}}(t) \exp\left[-j\gamma \left|E_{\mathrm{in}}(t)\right|^2\right] \tag{2}$$

where $E_{\mathrm{in}}(t)$ is the envelope of the incident electric field into the nonlinear fiber, and $E_{\mathrm{SPM}}(t)$ is the envelope of the output field. The parameter L is the length of the fiber, and γ is called the SPM coefficient. The variation in the phase of the signal introduces frequency shifting, i.e.,

$$\Delta\omega(t) = 2\pi\Delta f(t) = -\gamma L \frac{\partial \left|E_{\mathrm{in}}(t)\right|^2}{\partial t}. \tag{3}$$

This time-dependent frequency variation is also called frequency chirping, which broadens the signal's spectrum. In the case of an intense pulse traveling in a long fiber, this broadening can be considerable. It can sometimes exceed 100 THz, particularly when SPM is coupled with other nonlinear effects. Such extreme spectral broadening is referred to as the SC. Usually, dispersion is also important in the SC process. It has been recently reported [10] that the SC effect in a dispersion-flattened HNLF has been used as a nonlinear thresholding device for the SPE OCDMA system. The setup of the SC-based receiver is the same as the one shown in Fig. 3(b), but with the SPM fiber and optical power optimized for SC. When "1" is received, the rapid variation of the power of the recovered short pulse creates a strong broadening of the spectrum; therefore, a considerable amount of energy can pass through the optical low-pass filter (LPF) that follows the SPM fiber. In this paper, the LPF is modeled to have a cutoff frequency that rejects almost all energy of the original pulse and blue-shifted components and passes only the red-shifted frequencies. The low-intensity MAI signal's spectrum is broadened much less, and far less energy can go through the filter when "0" is received. Hence, a large contrast ratio can be observed at the output of the PD. Note that a high-pass optical filter, rather than a low-pass optical filter, can also be used; with the model of (2), the results are identical to the results presented here for an LPF.

III. Performance Analysis

If the pulse has a rectangular spectrum with bandwidth W, its electric-field amplitude can be represented by the equation

$$E_p(t) = \sqrt{P_0}\,\mathrm{sinc}\left(\frac{W}{2}t\right) \tag{4}$$

where P_0 is the peak power, and $\mathrm{sinc}\ x = \sin \pi x/(\pi x)$. The duration of the pulse is defined by $\tau_p = 2/W$. Reference [3] shows that, if random spreading sequences are used, the field of the coded signal can be approximated by a complex Gaussian random process with zero mean and variance P_0/N_0, where N_0 is the length of the spreading code. The duration of the encoded

signal is N_0 times the pulse duration, i.e., $N_0\tau_p$. Given this model of the light source, the performances of the SHG receiver (in the thin-crystal limit) and the SPM receiver are analyzed in the following two sections.

A. SHG Receiver

According to the receiver model described above, the decision statistic is essentially the energy of the SH signal within the response time of the electronics. In this paper, we set this response time to be equal to the duration of the encoded pulse $(N_0\tau_p)$. Suppose that, during some specific bit period, there are l interfering signals with data "1" and that random spreading codes are used. The field of the MAI after the decoder can be represented by

$$E_0(t) = A_R(t) + jA_I(t) \tag{5}$$

where A_R and A_I are independent Gaussian random processes with zero mean and variance $lP_0/2N_0$. When "0" is transmitted by the desired user, the field of the SH signal after the SHG crystal is given by

$$E_0^{(2)}(t) = E_0^2(t) = A_R^2(t) - A_I^2(t) + 2jA_R(t)A_I(t). \tag{6}$$

A thin crystal is assumed in this analysis; therefore, $E_0^{(2)}(t)$ is sent to the PD without any optical-filtering effect. The power of the SH signal, which is the output of the square-law converter, is given by

$$P_0^{(2)}(t) = \left|E_0^{(2)}(t)\right|^2 = \left(A_R^2(t) + A_I^2(t)\right)^2. \tag{7}$$

Respectively, the mean and variance of the SH signal power can be shown to be

$$\begin{aligned} E\left\{P_0^{(2)}(t)\right\} &= 8(lP_0/(2N_0))^2 \\ \mathrm{Var}\left\{P_0^{(2)}(t)\right\} &= 320(lP_0/(2N_0))^4. \end{aligned} \tag{8}$$

The decision statistic, which is the sampled value at the output of the integrator, is given by

$$X(''0'') = \int_A P_0^{(2)}(t)dt \tag{9}$$

where A denotes the interval of length T_r (the assumed response time) preceding the sample instant. The ensemble average of X is obtained by

$$E\{X|''0''\} = \int_A E\left\{P_0^{(2)}(t)\right\}dt = 8T_r(lP_0/(2N_0))^2. \tag{10}$$

The variance of the decision statistic can be obtained as follows. First, by definition, we have

$$\mathrm{Var}\{X|''0''\} = E\{X^2|''0''\} - E^2\{X|''0''\} \tag{11}$$

and

$$\begin{aligned} E\{X^2|''0''\} &= E\left\{\left(\int_A P_0^{(2)}(t)dt\right)^2\right\} \\ &= \int_{A\times A} E\left\{P_0^{(2)}(s)P_0^{(2)}(t)\right\}dsdt. \end{aligned} \tag{12}$$

Since the encoding and decoding processes only change the phases of the signal in various parts of the frequency domain, the power spectral density (PSD) of the MAI has the same shape as the spectrum of the original pulse, which is assumed to be rectangular with width W. Given that the mean power of the MAI is lP_0/N_0, the autocorrelation function of the MAI is a sinc function given by

$$R_{E_0}(t) = \frac{lP_0}{N_0}\,\mathrm{sinc}\left(\frac{W}{2}t\right). \tag{13}$$

By using the properties of Gaussian random variables [23] and (13), the autocorrelation of $P_0^{(2)}(t)$ can be shown to be

$$\begin{aligned} E\left\{P_0^{(2)}(s)P_0^{(2)}(t)\right\} &= 64\left(\frac{lP_0}{2N_0}\right)^4 \\ &\times\left\{\mathrm{sinc}^4\left[\frac{W}{2}(t-s)\right] + 4\,\mathrm{sinc}^2\left[\frac{W}{2}(t-s)\right] + 1\right\}. \end{aligned} \tag{14}$$

By using (14) in (12) and the fact that the sinc function is much narrower than the bit interval, we obtain

$$\sigma_0^2(l) = \mathrm{Var}\{X|''0''\} = 299\tau_p T_r(lP_0/(2N_0))^4. \tag{15}$$

The decision statistic is assumed to be Gaussian for data bit "0."

When "1" is sent by the desired transmitter, there will be a recovered short pulse $E_p(t)$ in addition to the noise-like MAI at the output of the decoder. The SH signal can be represented by

$$\begin{aligned} E_1^{(2)}(t) &= [E_0(t) + E_p(t)]^2 \\ &= E_p^2(t) + 2E_p(t)E_0(t) + E_0^{(2)}(t). \end{aligned} \tag{16}$$

The power of the SH signal is

$$\begin{aligned} P_1^{(2)}(t) &= \left|E_1^{(2)}(t)\right|^2 \\ &= E_p^4(t) + 4E_p^3(t)A_R + 2E_p^2(t)\left(3A_R^2 + A_I^2\right) \\ &\quad + 4E_p(t)A_R\left(A_R^2 + A_I^2\right) + \left(A_R^2 + A_I^2\right)^2. \end{aligned} \tag{17}$$

The decision statistic is given by

$$X(''1'') = \int_A P_1^{(2)}(t)dt. \tag{18}$$

Since most energy of the pulse resides in its main lobe, which has width τ_p, the other region is assumed to be unaffected by the

short pulse. Given these assumptions, the mean and variance of the decision statistic are shown to be

$$\begin{aligned} m_1(l) &= E\{X|''1''\} \\ &= E\{X|''0''\} + 2P_0^2\tau_p/3 + 4lP_0^2\tau_p/N_0 \\ \sigma_1^2(l) &= \mathrm{Var}\{X|''1''\} \\ &= \mathrm{Var}\{X|''0''\} + 9lP_0^4\tau_p^2/(2N_0) \\ &\quad + 44l^2P_0^4\tau_p^2/N_0^2 + 80l^3P_0^4\tau_p^2/N_0^3. \end{aligned} \tag{19}$$

The new terms come from the beating between the main lobe of the short pulse and the MAI. In most cases, the number of interfering users l is much smaller than N_0. Hence, unless the PD is extremely slow ($T_r/\tau_p \gg N_0$), the sum of the last three terms of $\sigma_1^2(l)$ in (19) is much greater than $\sigma_0^2(l)$. As a result, the system performance is dominated by these terms. Since $\sigma_0^2(l)$ and $\sigma_1^2(l)$ increase with larger T_r while $m_1 - m_0$ remain unchanged, a slower PD will still result in worse performance as expected. However, since the dominating factor does not change with T_r, the performance difference should be very small between PDs of different speeds.

Next, we examine the distribution of the decision statistic for data bit "1." From (16) and (17), it can be seen that the random process

$$\begin{aligned} r(t) &= \left[P_1^{(2)}(t)\right]^{1/4} \\ &= \left[\left(A_R(t) + E_p(t)\right)^2 + A_I^2(t)\right]^{1/2} \end{aligned} \tag{20}$$

is a Rician random variable within the main lobe of the pulse. Since the main lobe of the pulse dominates the behavior of the decision statistic, we approximate the distribution of $X(''1'')^{1/4}$ to be Rician, as well. Hence, the probability density function (PDF) of X is given by

$$f_{X|''1''}(x) = \frac{1}{4\sigma^2\sqrt{x}} \exp\left\{-\frac{1}{2}\frac{\sqrt{x}+\sqrt{A}}{\sigma^2}\right\} I_0\left(\frac{\sqrt[4]{A}x}{\sigma^2}\right) \tag{21}$$

where $A = 2P_0^2\tau_p/3$ and $\sigma^2 = \sqrt{A}3l/(4N_0)$ are picked to match the mean and variance given by (19). If the decision threshold is set to be $H = hP_0^2\tau_p$, the BER conditioned on the number of interfering users is given by

$$\begin{aligned} \Pr\{E|l\} &= \frac{1}{2}\left[Q\left(\frac{h - 2l^2/N_0}{l^2\sqrt{20/N_0^3}}\right) + 1 \right. \\ &\qquad \left. - Q\left(\frac{\sqrt[4]{A}}{\sigma}, \frac{\sqrt[4]{H}}{\sigma}\right)\right] \\ &= \frac{1}{2}\left[Q\left(\frac{h - 2l^2/N_0}{l^2\sqrt{20/N_0^3}}\right) + 1 \right. \\ &\qquad \left. - Q\left(\sqrt{\frac{4N_0}{3l}}, \sqrt[4]{\frac{2h}{3}}\sqrt{\frac{4N_0}{3l}}\right)\right] \end{aligned} \tag{22}$$

where the first Q function is the complementary cumulative distribution function of a standard Gaussian random variable, and the second one is the Marcum's Q function given by

$$Q(a,b) = \int_b^\infty x \exp\left[-\frac{(a^2+x^2)}{2}\right] I_0(ax)dx \tag{23}$$

where $I_0(\bullet)$ is the zeroth-order modified Bessel function of the first kind.

B. SPM Receiver

Based on the structure in Fig. 3(b), the decision statistic of the SPM-based receiver can be represented by the following equation:

$$\begin{aligned} X = \int_0^{f_{\mathrm{cut}}} \Big|\mathcal{F}\Big\{ &[E_0(t) + DE_p(t)] \\ &\times \exp\left[-j\gamma L\left|E_0(t) + DE_p(t)\right|^2\right] \Big\}\Big|^2 df \end{aligned} \tag{24}$$

where $E_0(t)$ is the electrical field of the MAI signal, which is modeled to be a complex Gaussian random process, as represented by (5). D represents the data bit from the desired user, and $E_p(t)$ is the field of the recovered short pulse when "1" is received. $\mathcal{F}\{\bullet\}$ represents the Fourier transform, and the outer norm-square is to obtain the energy spectrum. Because of the LPF, the decision statistic represents all the energy from the frequency zero up to the cutoff frequency f_{cut}.

When $D = 0$, only the MAI is present after the decoder. The autocorrelation function of the signal is given by (13). Reference [22] shows that if the input signal is Gaussian-distributed, the autocorrelation function of the output from the SPM fiber has the closed-form solution given by

$$R_{\mathrm{out}}(t) = \frac{R_{\mathrm{in}}(t)}{\left[1 + \left[\gamma L R_{\mathrm{in}}(0)\right]^2\left(1 - \left|\frac{R_{\mathrm{in}}(t)}{R_{\mathrm{in}}(0)}\right|^2\right)\right]^2} \tag{25}$$

where $R_{\mathrm{in}}(t) = R_{\mathrm{MAI}}(t)$ and $R_{\mathrm{out}}(t)$ are the autocorrelation functions of the input and output Gaussian random processes, respectively. Since $R_{\mathrm{in}}(0)$ is the mean power of the input signal, $\gamma L R_{\mathrm{in}}(0)$ represents the mean phase shift cause by the SPM. In general, the input autocorrelation function tends to decrease when $|t|$ increases from zero, and the denominator of (25) tends to increase. Hence, the autocorrelation function at the output is narrower than that of the input signal, and the spectrum at the output is wider than that of the input MAI. This is because the SPM effect scrambles the phase of the signal and decorrelates the Gaussian random process. By taking a Fourier transform, the broadened PSD of the MAI can be obtained. An integral of the PSD from zero to f_{cut} gives the mean power of the MAI after the LPF. When the data bit is "1," a short pulse is recovered after the decoder, as well as the MAI. The spectrum of the signal after the SPM fiber becomes too complicated to calculate

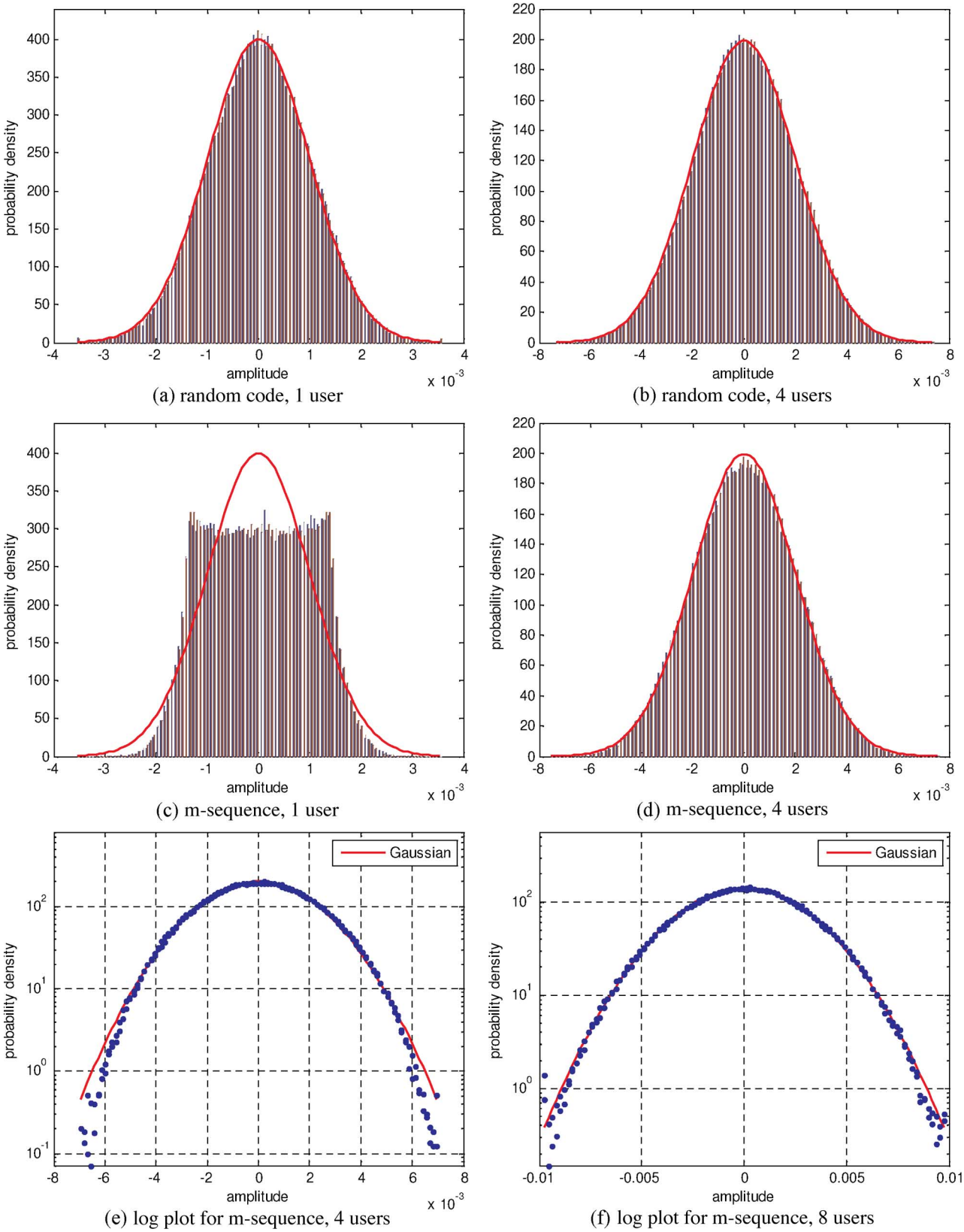

Fig. 4. PDFs of the amplitudes of encoded signals using 127-chip spreading sequences. Parts (a) and (b) correspond to binary random sequences. Parts (c)–(f) correspond to the m-sequence. Figures are obtained using the Monte Carlo method.

analytically. Numerical methods are used here to obtain the system performance for the SPM-based system. A threshold after the PD has to be set to determine if zero or one is sent by the desired transmitter. We note that, for the SPM receiver, there are two parameters that need to be optimized, i.e., the cutoff frequency and the decision threshold.

IV. Numerical Results

Since the nonlinear effects of the optical devices are extremely difficult to examine analytically, methods of numerical simulation are used here to determine the performances of the receivers discussed above. In the simulations, we first generate the waveforms of the short pulse and the MAI signals and then pass them to the nonlinear optical media and measure the output of the PD. Finally, using the Monte Carlo method, the decision statistic is compared with a threshold to estimate the data bit and calculate the BER. The shape of the ultrashort pulse is assumed to be a sinc function, as described by (4). The sampling frequency is set to be $20\pi \approx 62.8$ times the bandwidth of the pulse, which is high enough to avoid aliasing, even after SPM-induced broadening. The simulation of the nonlinear processing is done according to Fig. 3(a) and (b) for SHG and SPM, respectively. The PD is assumed to have a response time equal to the encoded-signal length $N_0\tau_p$.

First, the Gaussian approximation of the encoded signal is examined to determine if it is, indeed, a good assumption. The pulses are encoded using two kinds of different sequences for comparison. One is the m-sequence used in many experiments [12]–[14]. The other is the binary random sequence. Both sequences have a length of 127. The distributions of the amplitudes (both the real and the imaginary parts) of the encoded signals are shown in Fig. 4. The distributions of the m-sequence-encoded signals are obtained by averaging over all cyclic shifts of the sequence in the frequency domain. In Fig. 4(b) and (d)–(f), the relative delays and optical phases between different users are modeled to be uniformly distributed random variables. The results show that the random sequence results in a Gaussian-like signal, as expected in [3]. However, as shown in Fig. 4(c), the signal spread by the m-sequence is far from Gaussian. This is because the m-sequences have a deterministic spike-like autocorrelation function. By the Wiener–Khintchine Theorem, the power of a signal encoded by the m-sequences is almost a constant function of time, with some small fluctuations. The phase of the encoded signal has a uniform distribution over $[-\pi, \pi)$. Hence, the PDF of the real and imaginary parts of the encoded signal is a smoothed version of the PDF of the sine (or cosine) of a uniform distributed phase, which has [8] the form $1/(\pi\sqrt{1-x^2})$. Fig. 4(c) shows that its PDF is flat in the middle and has a much smaller tail than the Gaussian distribution. This more concentrated distribution results in less MAI and better performance than the randomly encoded signal, as shown in the performance simulation. Fig. 4(d)–(f) shows that, when the number of users increases, the Central Limit Theorem the comes into play, and the distribution of the overlapped signal approaches Gaussian very quickly. Therefore, the theoretical analyses for the SPE scheme should still hold for a large number of simultaneous interfering users (i.e., large l).

The bit-error probability of the SHG-based receiver that is conditioned on the number of interfering users is shown in Fig. 5. The system was simulated with both 127-chip binary random spreading sequences and the m-sequence with the same length. Different lengths of the walk-off effect are also tested. The performance of an ideal thresholder, followed by a PD

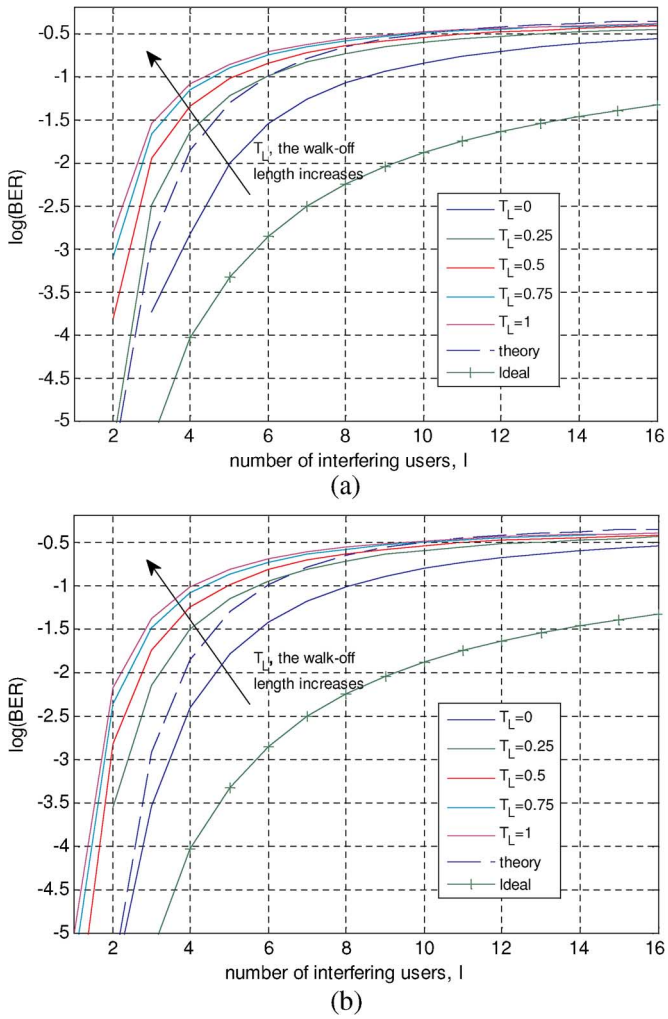

Fig. 5. BER of the SHG-based receiver conditioned on the number of interfering users. T_L is the ratio of the SHG walk-off length to the encoded signal length. (a) Conditional BER with 127-chip m-sequence. (b) Conditional BER with 127-chip binary random sequence.

and electronics with response time equal to the input pulse duration, is also shown with the label "ideal" for reference (this is the result from [3] with $\beta = 1$). The curves labeled "theory" are obtained by evaluating (22). Fig. 5 shows that the system performance decreases as the walk-off length increases. This is mainly because, if $E_1^{(2)}(t)$ in (16) is filtered, the electric field of the short pulse $E_p^2(t)$ is spread to a longer duration, which is proportional to the group velocity walk-off T_L. As a result, more beat noise is created in the power of the SH signal due to the beating between the spread pulse and the MAI. However, a thicker crystal with larger walk-off length has higher conversion efficiency, which results in more power in the SH signal. When the thermal and dark current noises are taken into account, there should be an optimal crystal length in the tradeoff between suppressing MAI and generating enough SH power to combat noise. It is also shown in Fig. 6 that the system employing the m-sequence as a spreading code has a better performance than the system using binary random sequences, particularly when the number of interferences is small. This is due to the smaller tail in the PDF of the MAI encoded with the m-sequence, as aforementioned.

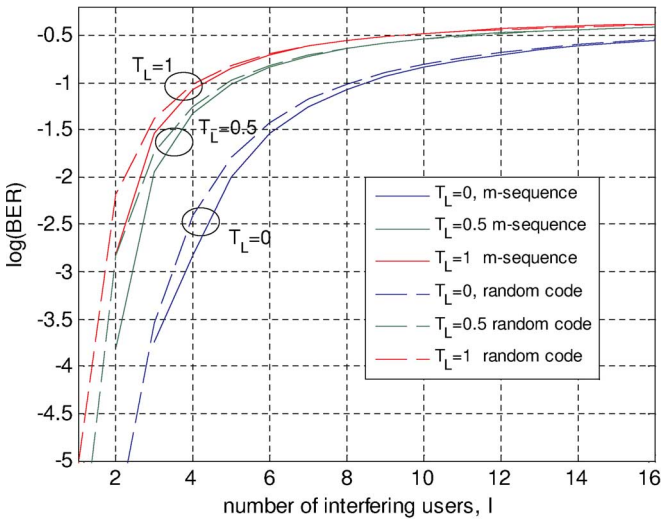

Fig. 6. Comparison between encodings with m-sequence and random sequences. The m-sequence encoded system has better performance because of the smaller tail of the PDF of the MAI. Both codes have length 127.

Jiang *et al.* [14] experimented with a 10-Gb/s SPE OCDMA system using the SHG receiver. They tested the BER with one interfering user overlapping with the recovered pulse from the desired user. In order to verify the accuracy of our simulation of the SHG receiver, we simulated the system with the same settings used by Jiang. The spreading code is the 31-chip m-sequence, and the SHG crystal has a walk-off length equal to the coded signal length. The simulated BER is 2.18×10^{-4}, which matches the measured data shown in [14, Fig. 4] very well.

Fig. 5 shows that the conditional BER ranges from 10^{-5} to 10^{-1} when the number of interferers varies from 2 to 16. This appears to result in poor performance. However, notice that not all simultaneous transmitters will interfere with the desired user for two reasons. First, some (roughly half) of them may transmit "0" and produce no interference. Second, the encoded-signal length may only be a small fraction of the bit duration. Therefore, if the total number of transmitting users is M and the ratio of bit duration to the coded-signal length is K, the number of interfering users I is a binomial random variable with parameters $(M-1, 1/(2K))$. The BER can be evaluated by applying the total probability formula

$$\Pr\{E\} = \sum_{l=0}^{M-1} \binom{M-1}{l} \left(\frac{1}{2K}\right)^{l} \left(1 - \frac{1}{2K}\right)^{M-1-l} \Pr\{E|l\}. \tag{26}$$

When K is large, the number of interfering users remains statistically small to get acceptable BER even with large M. For example, if $M = 50$ and $K = 50$, the expected value of I is only 0.5, and the variance is also 0.5. However, a large value of K decreases the bit rate if the light source and encoding scheme are fixed. The relation of the BER versus M is shown in Fig. 7. Equation (26) is used with K set to 100 and 50 to obtain the curves in the two figures. As expected, the system with a large value of K has a lower BER at the expense of a lower data rate. We can see that the theoretical curve obtained

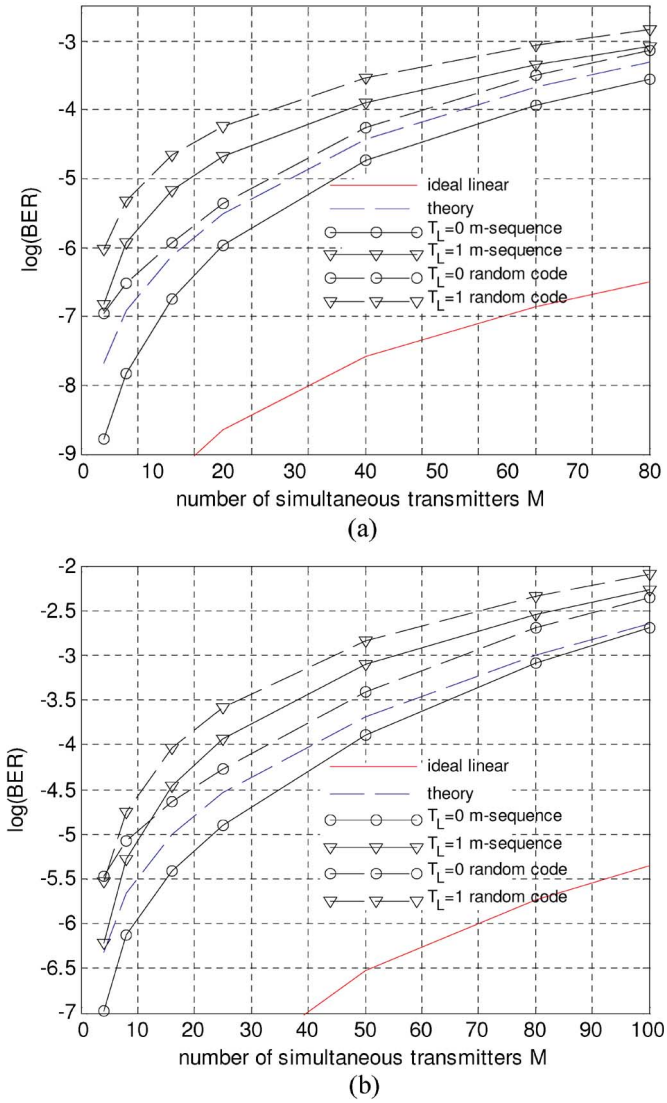

Fig. 7. BER of the SHG-based receiver versus the number of simultaneous transmitters. (a) BER versus $M(K = 100)$. (b) BER versus $M(K = 50)$.

from (22) matches well with the simulation results. Again, the performance decreases when the walk-off length increases. The best performance obtained with the SHG-based receiver is still several orders worse than the "ideal" receiver of [3].

For the SPM-based receiver, we simulated the system performance with three different strengths of the nonlinear effect. The maximum phase shifts $\phi_{\max} = \gamma L P_0$ at the peak of a pulse are 4.0π, 8.1π, and 16.2π for the three settings. The spreading-code length is set to $N_0 = 127$. Both the m-sequence and random sequences are examined. The broadened signal spectra are obtained using the Monte Carlo method and are shown in Fig. 8. The figure shows that, if a pulse is present in the signal after the decoder, the SPM-broadened bandwidth is much wider than that of MAI only. Fig. 8 also shows that larger $\phi_{\max}$ corresponds to wider broadening, as expected.

The cutoff frequency of the LPF and the decision threshold are jointly optimized by brute-force search to get the best performance. The BER conditioned on the number of interfering users is shown in Fig. 9. The curves of the SHG-based receiver and the ideal linear receiver are shown for comparison. This

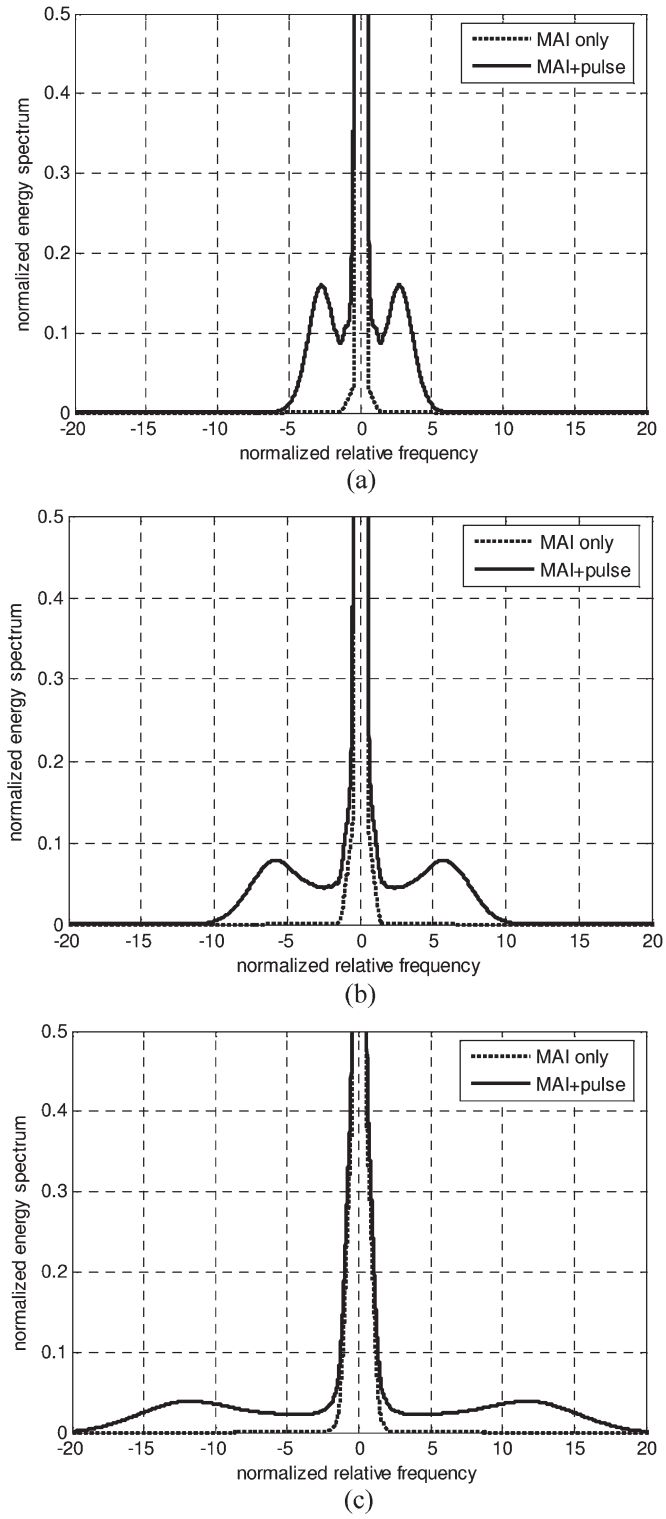

Fig. 8. Broadened signal power spectrum induced by the SPM effect. The horizontal axis is normalized with respect to the bandwidth of the short pulse; the vertical axis is normalized with respect to the height of the energy spectrum of a pulse. (a) Two interferences, $\phi_{\max} = 4.04\pi$. (b) Two interferences, $\phi_{\max} = 8.08\pi$. (c) Two interferences, $\phi_{\max} = 16.2\pi$.

figure shows that systems with stronger nonlinear effects have better performances, since a stronger SPM effect will spread the spectrum more and make it easier to discriminate the recovered pulse from MAI signals. One extreme is the SC thresholder reported in [10]. Considering the binomial distribution of the

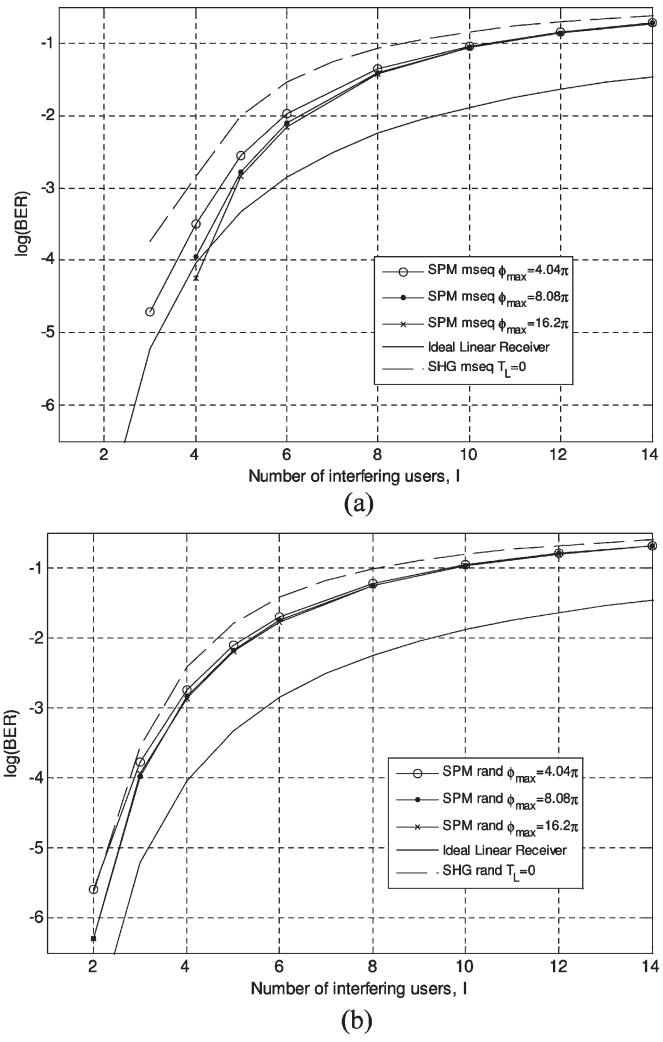

Fig. 9. BER of the SPM-based receiver conditioned on the number of interferers. (a) Performance of the SPM receiver using 127-chip m-sequence. (b) Performance of the SPM receiver using 127-chip random sequences.

number of interfering users, the performance curves are shown in Fig. 10 with $K = 100$ assumed in the simulation. Fig. 10 shows that, when the number of users is small, the SPM-based receiver using m-sequences can achieve better performance than the ideal receiver of [3] using binary random codes.

A performance comparison between the SHG receiver and the SPM receiver is shown in Fig. 11. It is shown that the former has a much higher BER. This is mainly because the intensity of the SH signal is essentially the fourth power of the electric field at the output of the decoder, which is the sum of the MAI and the recovered short pulse. The amplitude of the beat noise is about twice as strong as that of the fundamental signal. After convolution with the impulse response of the PD, the variance of the decision statistic is larger than that of the SPM receiver, and a larger BER results. However, the price paid for the better performance of the SPM receiver is larger power consumption. The SPM is only effective when the intensity of the optical signal is large enough. For example, in [24], where a 340-m-long fiber is used to create an SPM effect, the peak power is about 200 W, and even in [10], where the authors claim that their system uses the least power for this type of receiver,

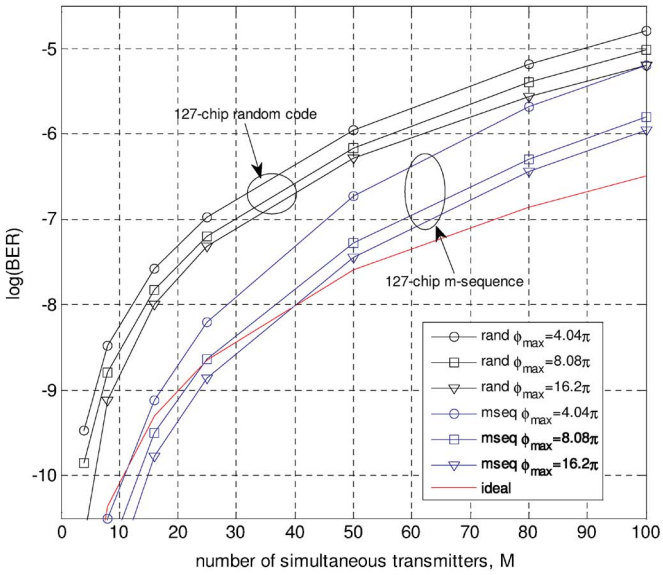

Fig. 10. BER of the SPM-based receiver versus the number of simultaneous transmitters ($K = 100$).

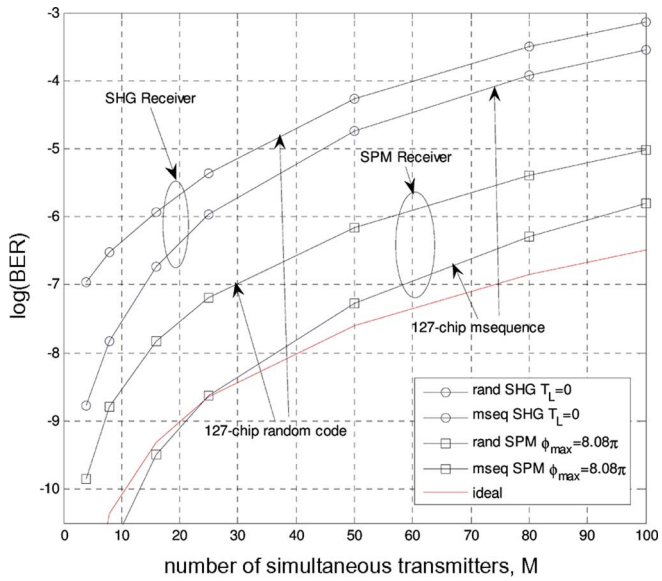

Fig. 11. Comparison between SHG and SPM receivers. $N_0 = 127$, and $K = 100$. The SHG receiver has much higher BER.

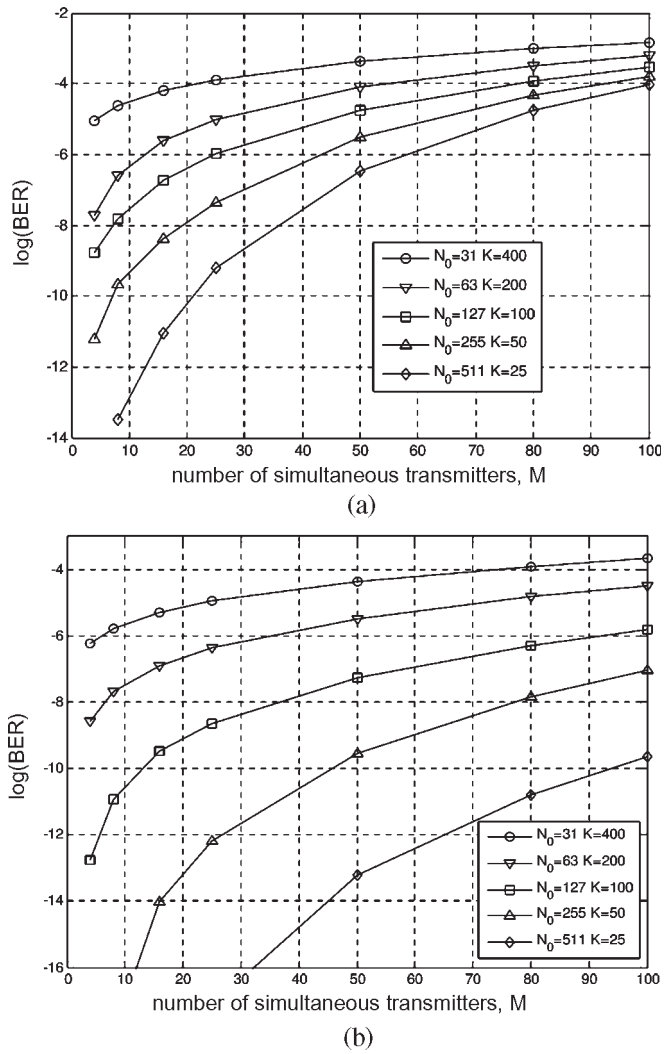

Fig. 12. Performances of the nonlinear receivers with fixed $N_0 \times K$. This figure suggests that when the pulse width and bit rate are fixed, a longer spreading code is desired to get a lower BER. (a) Performance of the SHG-based receiver with $N_0 \times K \approx 12\,700$. The spreading codes are m-sequences, and the walk-off length is $T_L = 0$. (b) Performance of the SPM-based receiver with $N_0 \times K \approx 12\,700$. The spreading codes are m-sequences, and the maximum phase shift is $\phi_{\max} = 8.08\pi$.

the peak power is about 6.3 W. The authors of [18] reported a similar peak power using HNLF as a thresholder. On the other hand, the system using the SHG receiver consumes much less power. It is reported in [14] that the energy in each 400-fs-long pulse is only 30 fJ, which corresponds to a peak power below 0.1 W, which is roughly two orders of magnitude better than the best known SPM-based receiver.

In these numerical results, we report on asynchronous systems. SHG systems with controlled timing have been examined in [25]. Where the adverse effects of beat noise can be eliminated, the SHG receiver with large group velocity walk-off ($T_L \gg 1$) can offer good performance [12]. In particular, in the multiple-user case with Hadamard coding, an SHG receiver, and $T_L \gg 1$, orthogonal waveform discrimination is reported in [25], provided that the transmission times of the encoded signals are carefully coordinated.

One important problem in communications is maximizing the system performance when both the bit rate and available bandwidth are fixed. In this ultrashort-pulse spectral-phase-encoding OCDMA system, bandwidth is determined by the reciprocal of the pulse duration; therefore, fixing bandwidth is equivalent to fixing the pulse duration. The encoded-signal length is approximately N_0 times the pulse duration, and the bit duration is assumed to be K times that of the encoded signal. If the bit rate is fixed, the product N_0K is fixed. When N_0 is large and K is small, the intensity of each interfering signal is low, but the number of interferers is likely to be large. On the other hand, if N_0 is small and K is large, the intensity of each interfering signal is high, but the number of interferers tends to be small. Reference [3] shows that, when the ideal receiver is used, larger N_0 is desired, i.e., the best performance is achieved when a long spreading code is used such that the encoded signal

extends over the whole bit duration. We also simulated the system performance with different N_0 and K while keeping $N_0K \approx 12\,700$. This means that, if the pulse duration is 400 fs, the bit rate for each user is about 200 Mb/s. The results are shown in Fig. 12. The figure shows that, for both the SHG receiver and the SPM receiver, a longer code is still desired in order to get better performance. When the spreading code length is 511, the BER is kept below 10^{-9} by the SPM-based receivers for 100 simultaneous transmitters, which is quite a remarkable performance.

V. Conclusion

An analysis of two nonlinear receivers based on the SHG and SPM effects is presented in this paper for the SPE OCDMA system. Both binary random sequences and m-sequences are examined. It is found that the signals encoded by m-sequences outperform those encoded by random sequences. The effect of the GVM-induced walk-off in SHG is studied, and a decrease of performance is shown as the walk-off length increases. An analytical result is derived to estimate the performance of the SHG-based receiver and is shown to match simulation results. The SPM-based receiver is simulated with different strengths of the nonlinear effect, and better performances are observed for stronger SPM effects. Comparisons show that the SPM-based receiver has a better performance than the SHG-based one, with the expense of larger power consumption. When the light source and the bit rate is fixed, longer spreading sequences provide lower BERs for both nonlinear receivers.

Acknowledgment

The authors would like to thank Dr. Z. Jiang for very helpful discussions.

References

[1] E. Marcom and O. G. Ramer, "Encoding–decoding optical fibre network," *Electron. Lett.*, vol. 14, no. 3, p. 48, Feb. 1978.

[2] N. Karafolas and D. Uttamchandani, "Optical fiber code division multiple access networks: A review," *Opt. Fiber Technol.*, vol. 2, no. 2, pp. 149–168, Apr. 1996.

[3] J. A. Salehi, A. M. Weiner, and J. P. Heritage, "Coherent ultrashort light pulse code-division multiple access communication systems," *J. Lightw. Technol.*, vol. 8, no. 3, pp. 478–491, Mar. 1990.

[4] S. Etemad, P. Toliver, R. Menendez *et al.*, "Spectrally efficient optical CDMA using coherent phase-frequency coding," *IEEE Photon. Technol. Lett.*, vol. 17, no. 4, pp. 929–931, Apr. 2005.

[5] P. C. Teh, M. Ibsen, J. H. Lee, P. Petropoulos, and D. J. Richardson, "Demonstration of a four-channel WDM OCDMA system using 255-chip 320-Gchips/s quaternary phase coding gratings," *IEEE Photon. Technol. Lett.*, vol. 14, no. 2, pp. 227–229, Feb. 2002.

[6] W. Naoya and K. Kitayama, "A 10 Gb/s optical code division multiplexing using 8-chip optical bipolar code and coherent detection," *J. Lightw. Technol.*, vol. 17, no. 10, pp. 1758–1765, Oct. 1999.

[7] A. M. Weiner, J. P. Heritage, and J. A. Salehi, "Encoding and decoding of femtosecond pulses," *Opt. Lett.*, vol. 13, no. 4, pp. 300–302, Apr. 1988.

[8] R. T. Hsu and J. S. Lehnert, "A characterization of multiple-access interference in generalized quadriphase spread-spectrum communications," *IEEE Trans. Commun.*, vol. 42, no. 234, pp. 2001–2010, Feb.–Apr. 1994.

[9] X. Wang, K. Matsushima, A. Nishiki, N. Wada, F. Kubota, and K.-I. Kitayama, "Experimental demonstration of 511-chip 640 Gchip/s superstructured FBG for high performance optical code processing," presented at the 30th European Conf. Optical Commun. (ECOC), Stockholm, Sweden, Sep. 2004, Paper Tu 1.3.7.

[10] X. Wang, N. Wada, T. Hamanaka, K.-I. Kitayama, and A. Nishiki, "10-user, truly-asynchronous OCDMA experiment with 511-chip SSFBG en/decoder and SC-based optical thresholder," in *Proc. Conf. Optic. Fiber Commun. (OFC)*, Los Angeles, CA, Mar. 2005.

[11] X. Wang, N. Wada, G. Cincotti, T. Miyzaki, and K. Kitayama, "Demonstration of 12-user, 10.71 Gbps truly asynchronous OCDMA using FEC and a pair of multi-port optical-encoder/decoders," presented at the 31st European Conf. Optical Commun. (ECOC), pp. 53–54, 2005, Paper Th 4.5.3.

[12] Z. Zheng and A. M. Weiner, "Spectral phase correlation of coded femtosecond pulses by second-harmonic generation in thick nonlinear crystals," *Opt. Lett.*, vol. 25, no. 13, pp. 984–986, Jul. 2000.

[13] Z. Jiang, D. S. Seo, S.-D. Yang, D. E. Leaird, R. V. Roussev, C. Langrock, M. M. Fejer, and A. M. Weiner, "Four-user, 2.5-Gb/s, spectrally coded OCDMA system demonstration using low-power nonlinear processing," *J. Lightw. Technol.*, vol. 23, no. 1, pp. 143–158, Jan. 2005.

[14] Z. Jiang, D. S. Seo, S.-D. Yang, D. E. Leaird, A. M. Weiner, R. V. Roussev, C. Langrock, and M. M. Fejer, "Four user, 10 Gb/s spectrally phase coded O-CDMA system operating at ~30 fJ/bit," *IEEE Photon. Technol. Lett.*, vol. 17, no. 3, pp. 705–707, Mar. 2005.

[15] H. P. Sardesai, C.-C. Chang, and A. M. Weiner, "A femtosecond code-division multiple-access communication system test bed," *J. Lightw. Technol.*, vol. 16, no. 11, pp. 1953–1964, Nov. 1998.

[16] R. P. Scott, W. Cong, C. Yang, V. J. Hernandez, N. K. Fontaine, J. P. Heritage, B. H. Kolner, and S. J. B. Yoo, "Error-free, 12-user, 10-Gb/s/user O-CDMA network testbed without FEC," *Electron. Lett.*, vol. 41, no. 25, pp. 1392–1394, Dec. 2005.

[17] R. P. Scott, W. Cong, V. J. Hernandez, K. B. Li, B. H. Kolner, J. P. Heritage, and S. J. B. Yoo, "An eight-user time-slotted SPECTS O-CDMA testbed: Demonstration and simulations," *J. Lightw. Technol.*, vol. 23, no. 10, pp. 3232–3240, Oct. 2005.

[18] R. P. Scott, W. Cong, K. B. Li, V. J. Hernandez, B. H. Kolner, J. P. Heritage, and S. J. B. Yoo, "Demonstration of an error-free 4×10 Gb/s multiuser SPECTS O-CDMA network testbed," *IEEE Photon. Technol. Lett.*, vol. 16, no. 9, pp. 2186–2188, Sep. 2004.

[19] W. Cong, R. P. Scott, V. J. Hernandez, K. B. Li, J. P. Heritage, B. H. Kolner, and S. J. B. Yoo, "High performance 70 Gb/s SPECTS optical-CDMA network testbed," *Electron. Lett.*, vol. 40, no. 22, pp. 1439–1440, Oct. 28, 2004.

[20] V. J. Hernandez, Y. X. Du, W. Cong, R. P. Scott, K. B. Li, J. P. Heritage, Z. Ding, B. H. Kolner, and S. J. B. Yoo, "Spectral phase-encoded time-spreading (SPECTS) optical code-division multiple access for terabit optical access networks," *J. Lightw. Technol.*, vol. 22, no. 11, pp. 2671–2679, Nov. 2004.

[21] G. Imeshev, M. A. Arbore, M. M. Fejer, A. Galvanauskas, M. Fermann, and D. Harter, "Ultrashort-pulse second-harmonic generation with longitudinally nonuniform quasi-phase-matching gratings: Pulse compression and shaping," *J. Opt. Soc. Amer. B, Opt. Phys.*, vol. 17, no. 2, pp. 304–318, Feb. 2000.

[22] G. P. Agrawal, *Nonlinear Fiber Optics*. New York: Academic, 1995, p. 549.

[23] J. W. Goodman, *Statistical Optics*. New York: Wiley, 1985, p. 44.

[24] H. P. Sardesai and A. M. Weiner, "Nonlinear fiber-optic receiver for ultrashort pulse code division multiple access communications," *Electron. Lett.*, vol. 33, no. 7, pp. 610–611, Mar. 1997.

[25] Z. Jiang, D. S. Seo, D. E. Leaird, A. M. Weiner, R. V. Roussev, C. Langrock, and M. M. Fejer, "Multi-user, 10 Gb/s spectrally phase coded O-CDMA system with hybrid chip and slot-level timing coordination," *IEICE Electron. Express*, vol. 1, no. 13, pp. 398–403, 2004.

Bin Ni received the B.Eng. degree in electronic engineering from Tsinghua University, Beijing, China, in 2000 and the Ph.D. degree in electrical and computer engineering from Purdue University, West Lafayette, IN, in 2005.

He was a Research Assistant with the Spread Spectrum and Satellite Communications Research Laboratory, Purdue University. He is now with Marvell Semiconductor, Santa Clara, CA as a Senior Design Engineer. His research interests are in spread-spectrum communication, optical communication, storage systems, and digital-signal processing.

James S. Lehnert (S'83–M'84–SM'95–F'00) received the B.S. (with the highest honors), M.S., and Ph.D. degrees in electrical engineering from the University of Illinois, Urbana–Champaign, in 1978, 1981, and 1984, respectively.

From 1978 to 1984, he was a Research Assistant at the Coordinated Science Laboratory, University of Illinois. He was a University of Illinois Fellow from 1978 to 1979 and an IBM Predoctoral Fellow from 1982 to 1984. He has held summer positions with the Data Systems Research Laboratory, Motorola Communications, Schaumburg, IL, and with the Advanced Technology Department, Harris Corporation, Melbourne, FL. He is currently a Professor with the School of Electrical and Computer Engineering, Purdue University, West Lafayette, IN, where he is currently a Purdue University Faculty Scholar. His current work is in communication and information theory, with emphasis on spread-spectrum communications.

Dr. Lehnert has served as Editor for Spread Spectrum for the IEEE TRANSACTIONS ON COMMUNICATIONS and as Guest Editor for the IEEE JOURNAL ON SELECTED AREAS IN COMMUNICATIONS.

Andrew M. Weiner (S'84–M'84–SM'91–F'95) received the Sc.D. degree in electrical engineering from Massachusetts Institute of Technology, Cambridge, in 1984.

Upon graduation, he was with Bellcore, first, as a member of the Technical Staff and, later, as the Manager of Ultrafast Optics and Optical Signal Processing Research. In 1992, he was with Purdue University, West Lafayette, IN, where he is currently the Scifres Distinguished Professor of electrical and computer engineering. His research focuses on ultrafast-optics signal processing and applications to high-speed optical communications and ultrawideband wireless. He is particularly well known for his pioneering work in the field of femtosecond pulse shaping, which enables generation of nearly arbitrary ultrafast optical waveforms according to user-specification. He has published six book chapters and over 190 journal articles. He has been the author or coauthor of over 300 conference papers, including approximately 80 conference invited talks, and has presented over 70 additional invited seminars at university, industry, and government organizations. He is the holder of nine U.S. patents.

Prof. Weiner is a Fellow of the Optical Society of America and has won numerous awards for his research. He has served as Cochair of the Conference on Lasers and Electro-optics and the International Conference on Ultrafast Phenomena and as Associate Editor of several journals. He has also served as a Secretary/Treasurer of the IEEE Lasers and Electro-Optics Society and as a Vice President of the International Commission on Optics.